ACS SyntheticBiology

Letter

pubs.acs.org/synthbio

Rapid and Inexpensive Evaluation of Nonstandard Amino Acid Incorporation in *Escherichia coli*

Jordan W. Monk, Sean P. Leonard, Colin W. Brown, Michael J. Hammerling, Catherine Mortensen, Alejandro E. Gutierrez, Nathan Y. Shin, Ella Watkins, Dennis M. Mishler,* and Jeffrey E. Barrick*

Center for Systems and Synthetic Biology, Department of Molecular Biosciences, The University of Texas at Austin, Austin, Texas 78712, United States

Supporting Information

ABSTRACT: By introducing engineered tRNA and aminoacyl-tRNA synthetase pairs into an organism, its genetic code can be expanded to incorporate nonstandard amino acids (nsAAs). The performance of these orthogonal translation systems (OTSs) varies greatly, however, with respect to the efficiency and accuracy of decoding a reassigned codon as the nsAA. To enable rapid and systematic comparisons of these critical parameters, we developed a toolkit for characterizing any *Escherichia coli* OTS that reassigns the amber stop codon (TAG). It assesses OTS performance by comparing how the fluorescence of strains carrying plasmids encoding a fused RFP-GFP reading frame, either with or without an intervening TAG codon, depends on the presence of the nsAA. We used this kit to (1) examine nsAA incorporation by seven different OTSs, (2) optimize nsAA concentration in growth media, (3) define the polyspecificity of an OTS, and (4) characterize evolved variants of amberless *E. coli* with improved growth rates.

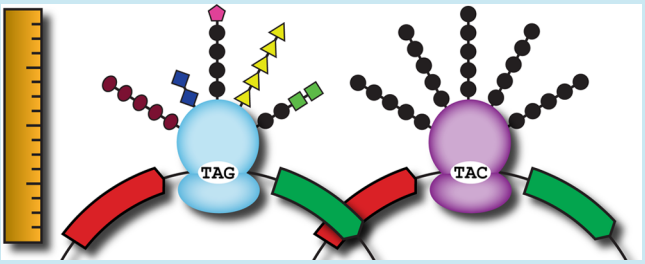

KEYWORDS: *expanded genetic code, noncanonical amino acid, unnatural amino acid, amber suppressor tRNA, nsAA measurement kit*

One goal of synthetic biology is to improve upon the limited chemical alphabets utilized by living organisms.[1] The development of orthogonal translation systems (OTSs) has enabled a variety of nonstandard amino acids (nsAAs) to be incorporated into proteins *in vivo*.[2,3] Many of these nsAAs can be used to create cells with novel capabilities. For example, some contain functional groups that enable halogen bonds[4,5] or disulfide bonds[6] with unusual properties compared to the interactions that normally stabilize protein structures. Other nsAAs can be used for bioorthogonal click chemistry,[7] photo-cross-linking,[8] or photocleavage[9] to further diversify the chemistry of cells and to exert precise spatiotemporal control of protein function.

Artificially expanding the genetic code is typically accomplished by expressing a new tRNA and aminoacyl-tRNA synthetase (aaRS) pair in a host cell.[2,3] In this setup, the additional aaRS has been engineered to recognize the nsAA and charge it onto the new tRNA. In *E. coli*, this tRNA is usually mutated so that it decodes the amber codon (TAG) as the nsAA. Recently, the functionality of OTSs has been further improved by deleting the protein release factor that competes with nsAA incorporation at the amber codon,[10] engineering a protein elongation factor to better accommodate the OTS tRNA,[11] and new methods for OTS directed evolution.[12,13]

The performance of an OTS can be defined in terms of two main parameters, fidelity and efficiency.[3,14,15] Fidelity refers to the accuracy with which the reassigned codon is read by the ribosome as the nsAA *versus* misread as any other amino acid. A lower fidelity OTS will result in proteins with mixture of the nsAA and one or more other amino acids at each TAG codon. Efficiency reflects how quickly the ribosome is able to read through the reassigned codon. A less efficient nsAA-incorporation system will result in a lower yield of output protein. The fidelity and efficiency of an OTS depend on many factors, including the rate of import of the nsAA into the host cell, the specificity of tRNA charging by the novel aaRS, and how effectively the new tRNA binds to and is translocated by the ribosome when it encounters the reassigned codon.[14] While these performance metrics are both derived from the biochemical properties of a particular orthogonal tRNA/aaRS pair, they are also somewhat independent, such that an OTS with low translational efficiency may still have very high fidelity, for example.

OTS performance is typically assessed by expressing GFP or another reporter protein from an open reading frame containing one or more copies of the reassigned codon.[13,16] Efficiency is judged by comparing the yield of this full-length reporter protein—monitored *via* a band on a gel, fluorescence, or enzyme activity—to a control gene with no copies of the reassigned codon. Fidelity is assessed by performing mass spectrometry on purified protein samples or by measuring

Received: July 11, 2016
Published: September 20, 2016

DOI: 10.1021/acssynbio.6b00192
ACS Synth. Biol. 2017, 6, 45−54

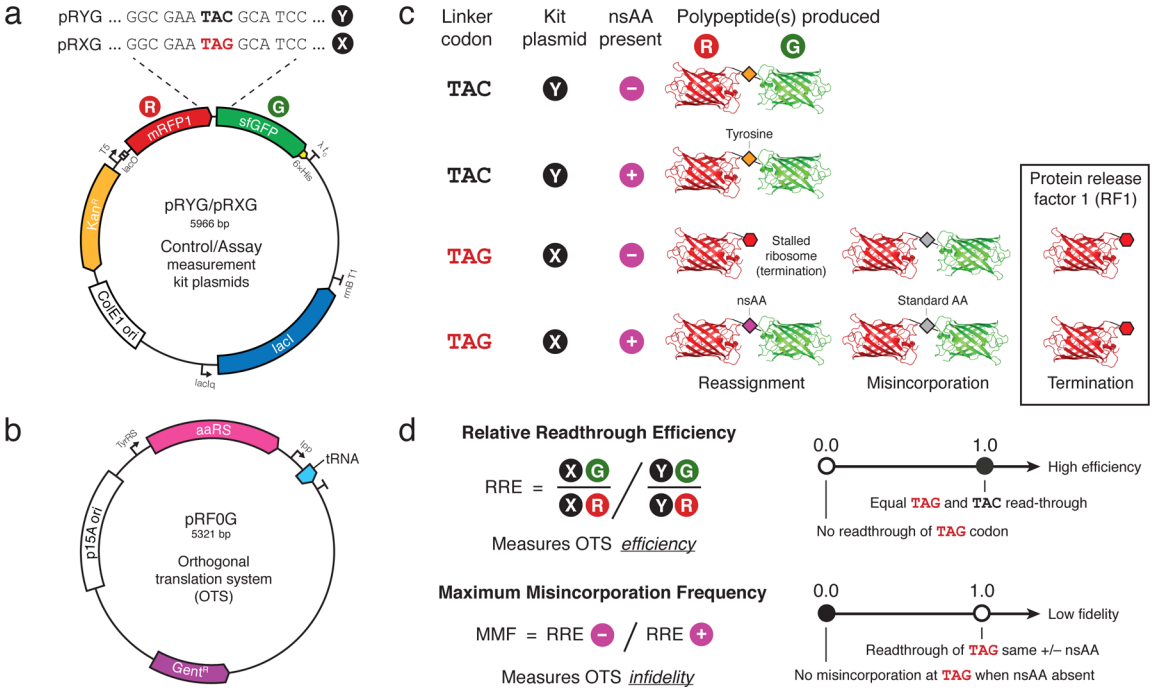

Figure 1. Measurement kit for nsAA incorporation systems. (a) The pRYG (control) and pRXG (assay) plasmids both encode an RFP-GFP fusion protein if a linker sequence is translated without stopping. They differ only in a single linker codon that is either a canonical tyrosine codon (TAC) or an amber codon (TAG) that has been reassigned to a nonstandard amino acid (nsAA). (b) The pRF0G plasmid expresses the aminoacyl-tRNA synthetase enzyme and the cognate amber-decoding tRNA that together constitute an orthogonal translation system (OTS) for expanding the genetic code with a particular nsAA. (c) This table shows the scenarios leading to the expression of each fluorescent protein from pRYG (Y) and pRXG (X) when the nsAA coded for by the TAG amber codon is present *versus* absent in the growth medium. In the amberless *E. coli* C321.ΔA.exp host strain used in this study, protein release factor 1 (RF1) was deleted, so the boxed mechanism for terminating translation does not compete with nsAA incorporation at the TAG codon. (d) Formulas for relative readthrough efficiency and maximum misincorporation frequency. These parameters characterize OTS efficiency and fidelity, respectively, as described on the scales shown on the right.

protein yield from the recoded gene in the absence of the nsAA. While the first study creating a new OTS for a given nsAA typically characterizes the performance of several closely related aaRS and/or tRNA variants, OTSs derived from different studies or for incorporating different nsAAs are rarely compared in the same host cells under uniform growth conditions. Furthermore, there is no easy way for nonexperts to cheaply and rapidly perform these measurements to ensure that an OTS is functioning in their hands or to screen many growth conditions to optimize OTS performance. Therefore, we designed and tested a genetic toolkit that can be used to assess the function of an OTS strictly from fluorescent read-out.

RESULTS AND DISCUSSION

Assessing Orthogonal Translation System Performance. Our method uses two reporter plasmids to measure the fidelity and efficiency of *in vivo* nsAA incorporation in *E. coli* (Figure 1a). Each plasmid encodes mRFP1 and sfGFP fused into a single reading frame *via* a flexible peptide linker. In the control plasmid, pRYG, the DNA sequence encoding the linker contains a TAC tyrosine codon. The assay plasmid, pRXG, is identical except for a single point mutation that converts the TAC into a TAG amber codon to direct incorporation of the nsAA by the OTS. In this configuration, GFP signals readthrough of the focal TAC/TAG codon, and RFP serves as an internal control for any variance in overall protein production. Each version of the mRFP1-sfGFP fusion is terminated by a TAA stop codon after a C-terminal 6 × His tag that can be used to purify the protein for mass spectrometry.

To use the nsAA measurement kit, the control (pRYG) and assay (pRXG) plasmids are transformed separately into an *E. coli* strain containing an orthogonal translation system that recodes the amber codon to a nonstandard amino acid. In this study, each OTS consisted of an aaRS-tRNA pair encoded on plasmid pRF0G (Figure 1b), and we tested OTS function in the genomically recoded "amberless" *E. coli* strain C321.ΔA.exp.[10] Performance of an OTS is evaluated by measuring RFP and GFP fluorescence (normalized to OD600) under four conditions: (1) assay plasmid with nsAA, (2) assay plasmid without nsAA, (3) control plasmid with nsAA, and (4) control plasmid without nsAA (Figure 1c).

The pRYG plasmid is a control for the relative GFP/RFP fluorescence signal expected for the entire fusion protein when there is efficient readthrough as a standard amino acid at this linker position. Therefore, the relative readthrough efficiency (RRE) of the TAG codon is the GFP/RFP fluorescence ratio for the pRXG assay plasmid divided by the GFP/RFP fluorescence ratio for the pRYG control plasmid (Figure 1d). For an efficient aaRS-tRNA pair, the RRE when the nsAA is present in the media should approach or surpass a value of one, as this metric reflects how well the TAG amber codon is translated compared to the TAC tyrosine codon.

RRE values do not contain any information about what amino acid is incorporated at the TAG codon, only how efficiently this codon is translated. The fidelity of an OTS is evaluated by comparing the RRE values obtained with and

DOI: 10.1021/acssynbio.6b00192
ACS Synth. Biol. 2017, 6, 45−54

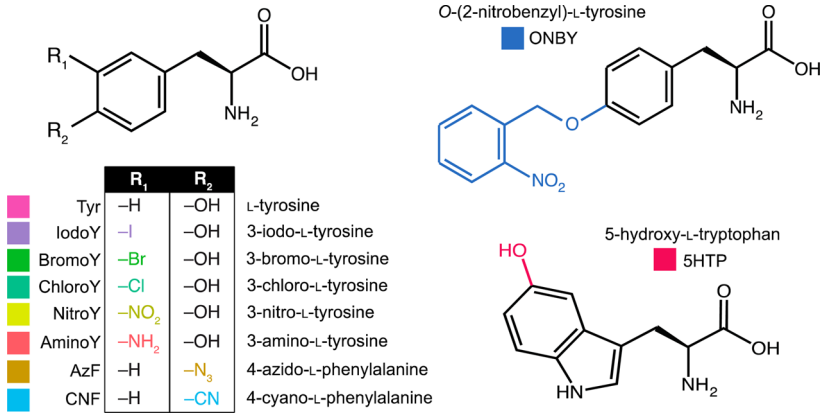

Figure 2. Nonstandard amino acids used in this study.

Table 1. Orthogonal Translation Systems Tested

aaRS[a]	tRNA[b]	amino acid	mutations	reference
Tyr	Nap3	L-tyrosine	None	16
AminoY	Nap3	3-amino-L-tyrosine	Y32Q, L65E, F108G, Q109L, D158S, L162Y	35
NitroY	Nap3	3-nitro-L-tyrosine	Y32R, H70L, Q155M, D158G, I159L, L162H	36
IodoY	Nap3	3-iodo-L-tyrosine	H70A, D158T, I159S, D286Y	4
ONBY	Nap3	*O*-(2-nitrobenzyl)-L-tyrosine	Y32G, L65G, F108E, D158S, L162E	9
AzF	Nap3	4-azido-L-phenylalanine	Y32T, E107N, D158P, I159L, L162Q	19
CNF	Nap3	4-cyano-L-phenylalanine	Y32L, L65V, F108W, Q109M, D158G, I159A	37
5HTP	AS3.4−40A	5-hydroxy-L-tryptophan	T107C, P254T and C255A	12

[a]All aaRSs except 5HTP are derived from the *Methanocaldococcus jannaschii* tyrosyl-tRNA synthetase (Tyr). 5HTP is derived from the *Saccharomyces cerevisiae* tryptophanyl-tRNA synthetase. [b]All systems except 5HTP were tested with the same Nap3 tRNA variant.[32]

without nsAA present. Specifically, an (in)fidelity metric, the maximum misincorporation frequency (MMF), is calculated by dividing the RRE when nsAA is not added to the growth media by the RRE when nsAA is present (Figure 1d).

An ideal OTS has an MMF value of zero, reflecting that no GFP is produced unless the nsAA is present. Note, however, that MMF is a very strict measure of fidelity. Some engineered aaRS-tRNA pairs are known to incorporate mostly the nsAA when it is provided at a sufficiently high concentration, but to nonspecifically charge the tRNA with a standard amino acid instead when it is more abundant.[12,15] Similarly, in the amberless *E. coli* host used in our experiments, translation is able to proceed to some extent through a single TAG codon, even when no cognate tRNA from an OTS is present.[10] Presumably, this readthrough occurs because there is no other fate for ribosomes stalled on an amber codon except mistranslation by a noncognate tRNA or very slow dissociation, because release factor 1 is deleted in this strain. Thus, MMF should be interpreted as an upper bound on how often the TAG codon is incorrectly decoded as a standard amino acid.

Comparing Orthogonal Translation Systems. We first used the kit to evaluate how well different nsAAs (Figure 2) were incorporated into proteins by a panel of different OTS systems (Table 1), most derived from the *Methanocaldococcus jannaschii* tyrosine aaRS-tRNA pair. Time courses of OD600, RFP, and GFP signals were collected during growth of cells with each OTS and kit plasmid in LB media. For test conditions with nsAA present, it was added a concentration of 250 μM. We initially validated these measurements by examining the 3-iodotyrosine (IodoY) system, which we have found to have high fidelity and efficiency in previous studies.[17,18] For the IodoY system, there is a large increase in GFP fluorescence for the pRXG assay plasmid when 3-iodotyrosine is present *versus* when it is absent in mid log phase (Figure 3a), as is expected for a system with high fidelity. The GFP signal also reaches similar levels for pRXG and the pRYG control plasmid when nsAA is present, which indicates 3-iodotyrosine is incorporated at the TAG codon with a similar efficiency to that of tyrosine at TAC. After cells have reached a saturating OD600, the specificity of the system appears to go down and GFP signal from the assay plasmid eventually increases in the condition lacking nsAA, which may indicate that misincorporation begins to occur at TAG during stationary phase.

The time-course data collected for IodoY and three other tRNA-aaRS systems are representative of the variation in OTS performance that we observed. The AminoY OTS efficiently reads through the TAG codon (yielding GFP signal), whether or not the nsAA 3-aminotyrosine is provided (Figure 3b). Thus, while it efficiently translates the amber codon, it has low fidelity and is expected to often decode TAG as amino acids other than the nsAA under our test conditions. NitroY exemplifies a third case (Figure 3c). For this OTS, the signal of GFP from the assay plasmid is greater in the presence of nsAA than when it is not provided, but it does not reach anywhere near the level of control plasmid. Thus, the NitroY OTS accurately decodes TAG as 3-nitrotyrosine but with a very low translational efficiency. Finally, the function of the AzF system is very similar to that of the IodoY system (high efficiency and fidelity), except the fidelity of this OTS appears to remain high even after cells transition into stationary phase.

To succinctly compare OTS performance, we present the rest of our measurements as the average RRE and MMF values over a time window when the cultures were in mid log phase

DOI: 10.1021/acssynbio.6b00192
ACS Synth. Biol. 2017, 6, 45−54

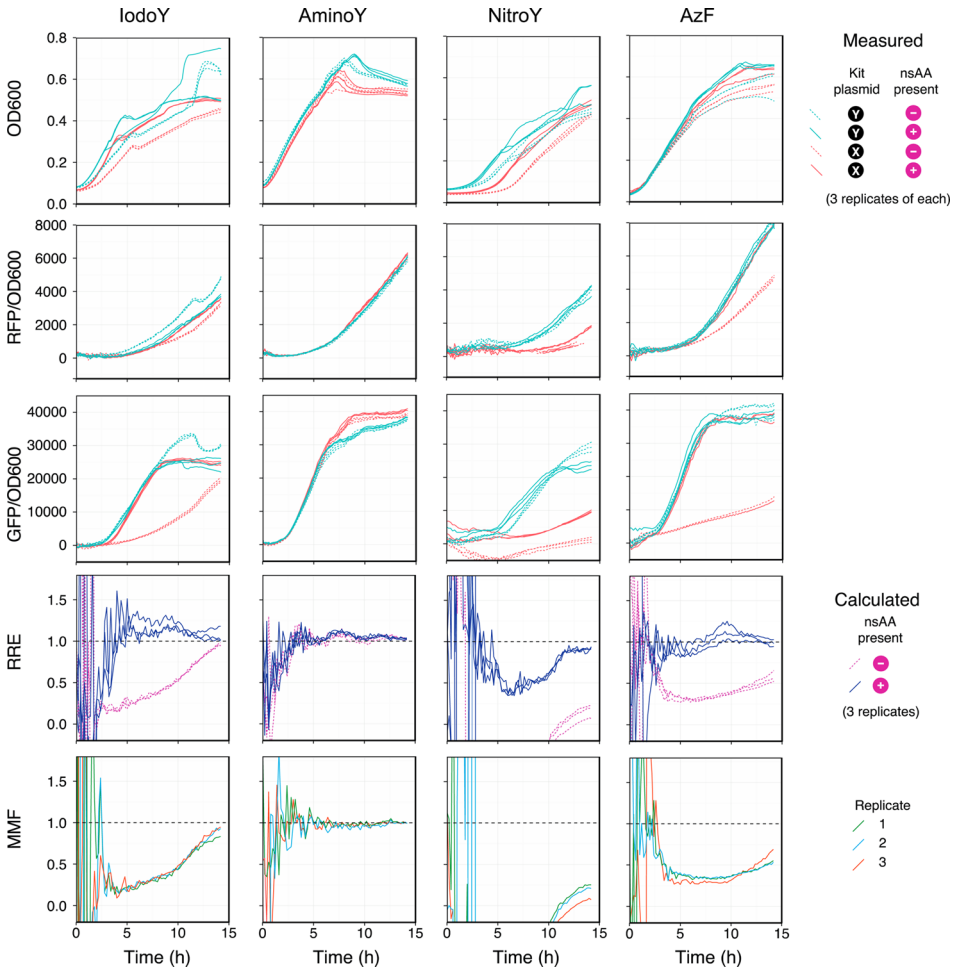

Figure 3. Characterization of four orthogonal translation systems. The top three rows show OD600, RFP/OD600, and GFP/OD600 signals over time for cells with an OTS plasmid, either the pRYG or pRXG kit plasmid, and with or without the nsAA present. The bottom two rows show the relative readthrough efficiency (RRE) and maximum misincorporation frequency (MMF) values calculated from these readings according to the equations in Figure 1d. Higher RRE values reflect more efficient translation of the reassigned TAG codon by the OTS, with a value of 1.0 equating to readthrough of the TAC tyrosine codon by the native translational machinery. Lower MMF values correspond to higher OTS fidelity. The MMF is 1.0 when there is no apparent specificity for incorporating the nsAA because readthrough of the TAG codon is equally efficient whether the nsAA is provided in the growth media or not.

(Figure 4a). We tested the Tyr OTS, which most of these nsAA systems are derived from, as an additional positive control. Like the IodoY system, it decodes TAG as efficiently as the TAC codon is translated as tyrosine by the native aaRS and tRNA pair (RRE value of ∼1.0). We found that two of the three remaining OTSs for incorporating nsAAs functioned well, while one did not. The ONBY and 5HTP systems exhibit intermediate RRE and MMF values. Both have very low readthrough efficiencies for TAG when the nsAA is present, but they appear to maintain significantly better accuracy for nsAA incorporation than the AminoY system. Finally, the CNF system exhibits very low fidelity, much like the AminoY OTS, under our assay conditions.

To better understand the relationship between the maximum misincorporation frequency (MMF) value measured by our kit and OTS fidelity, we employed protein mass spectrometry. Samples of the mRFP1-sfGFP fusion protein expressed in the presence of nsAA from the assay plasmid were purified from mid log phase cultures of cells containing either the Tyr, IodoY, AminoY, NitroY, or CNF aaRS-tRNA systems. In comparison to the Tyr OTS control (Figure S1), the mass peaks found in the IodoY (Figure S2) and NitroY (Figure S3) systems indicated that >95% of full-length proteins incorporated nsAA at the amber codon. This result for IodoY stresses how MMF establishes only a maximal limit on OTS infidelity (in this case, <30% misincorporation), but the true accuracy of translation when the nsAA is provided may be higher. On the other hand, we did not detect a mass peak corresponding to the expected nsAA-containing products for either the AminoY (Figure S4) or CNF (Figure S5) systems. Thus, the poor MMF values of ∼1.0 for these systems reflect that they are mostly incorporating tyrosine instead of the nsAA at TAG. Each of the aminoacyl-tRNA synthetases that we tested has been used to successfully incorporate its cognate nsAA with high fidelity in previous studies. The discrepancies in which poorer performance was found in our experiments are likely due to the use of different culture conditions (*e.g.*, minimal media instead of LB), *E. coli* strains (*e.g.*, hosts containing intact RF1 genes), or OTS configurations (*e.g.*, different plasmid arrangements or tRNA variants).

Effect of Varying Nonstandard Amino Acid Concentration. Many interesting and useful nsAAs are extremely expensive or are only available in limited quantities because they must be custom-synthesized by the laboratories that use

DOI: 10.1021/acssynbio.6b00192
ACS Synth. Biol. 2017, 6, 45−54

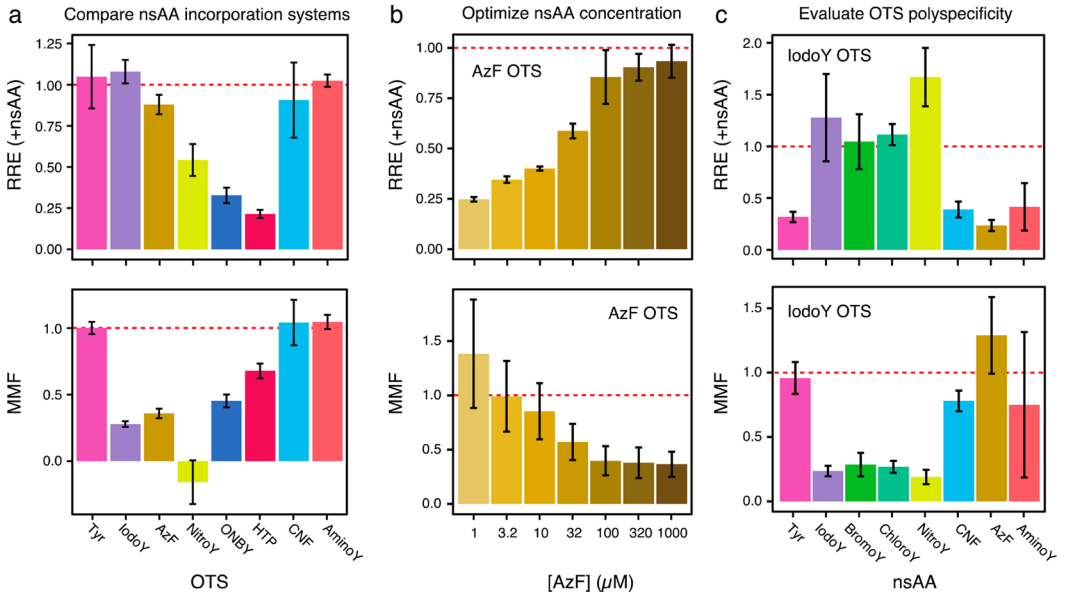

Figure 4. Applications of the nsAA measurement kit. In each panel, data from mid log phase in a time course as in Figure 3 were averaged to produce one summary value of RRE and MMF. Error bars are estimated 95% confidence intervals (see Methods). Nonstandard amino acids and orthogonal translation systems are abbreviated as in Table 1. (a) Comparison of OTS system function with 250 μM of their cognate nsAAs. (b) Function of the AzF OTS with different concentrations of 3-azidophenylalanine. (c) Incorporation of different nsAAs by the IodoY OTS when provided at 250 μM.

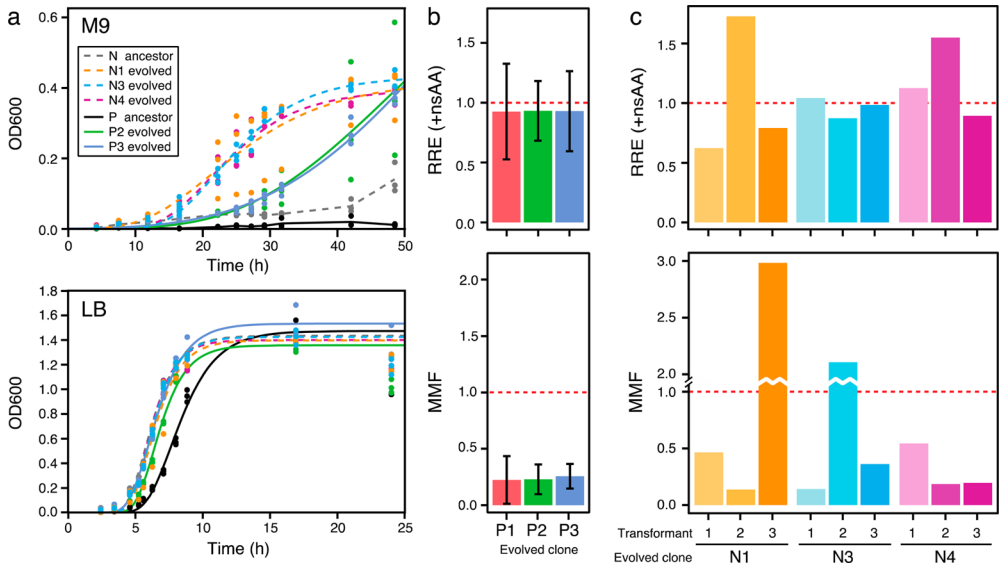

Figure 5. Characterization of variants of amberless *E. coli* strain C321.ΔA.exp evolved for more rapid growth. (a) Growth curves in M9 (top panel) or LB (bottom panel) medium for ancestral strains without (N0) and with (P0) the IodoY OTS plasmid compared to three strains evolved without any plasmid (N1, N3, and N4) and two strains evolved with the OTS plasmid (P2 and P3). Dashed and solid lines indicate strains without or with the OTS plasmid, respectively. Curves are fits to OD600 in three replicate cultures to a modified Gompertz function,[34] except the curves for strains P and N in M9, which are linear interpolations. Strains were grown to saturation in LB before being transferred to the growth medium being tested. (b) Performance of the IodoY OTS in three strains evolved with the OTS plasmid present (P1, P2, P3) evaluated using the nsAA measurement kit as in Figure 4. Error bars are 95% confidence intervals estimated from three replicates. (c) Performance of the IodoY OTS in the three strains evolved without any OTS plasmid present (N1, N2, N3). For each strain, three different transformants of the OTS plasmid were evaluated using the nsAA measurement kit with one biological replicate per transformant.

them. Therefore, one often wants to add only the minimum amount of nsAA to a culture that is needed to ensure accurate and efficient translation of the reassigned codon. 4-azidophenylalanine is one of the more costly nsAAs that we tested, so we measured performance of this OTS at AzF concentrations ranging from 1 μM to 1 mM (Figure 4b). We found that the efficiency and fidelity of this OTS was equal at all nsAA concentrations ≥100 μM. Therefore, we conclude that significantly less AzF is needed for this OTS than the 250 μM concentration that we used in our initial experiments and the 1 mM or higher that is typically used in other studies.[19,20]

Characterizing Orthogonal Translation System Polyspecificity. Several OTS systems have been reported to exhibit polyspecificity, meaning that they can be used to incorporate different nsAAs into proteins depending on which one is present in the growth medium, while not incorporating

DOI: 10.1021/acssynbio.6b00192
ACS Synth. Biol. 2017, 6, 45−54

Table 2. Mutations in Evolved Variants of Amberless *E. coli* Strain C321.ΔA.exp

clone	position	mutation	annotation	gene	description
N3	49 801	A → T	promoter (−23 bp)	*folA*	dihydrofolate reductase
P3	49 809	$(T)_{8\rightarrow7}$	promoter (−15 bp)	*folA*	dihydrofolate reductase
N1	50 091	G → A	E90K (GAA → AAA)	*folA*	dihydrofolate reductase
N4	50 222	G → A	W133* (TGG → TGA)	*folA*	dihydrofolate reductase
P2	50 283	G → C	E154Q (GAG → CAG)	*folA*	dihydrofolate reductase
P3	158 749	C → T	R70H (CGC → CAC)	*pcnB*	polyA polymerase I
P2	158 937	$(A)_{5\rightarrow6}$	frameshift (21/1398 bp)	*pcnB*	polyA polymerase I
N1	4 356 064	G → A	A192A (GCC → GCT)	*lysU*	lysine tRNA synthetase, inducible
P2	4 445 946	C → A	V548V (GTC → GTA)	*tamA*	translocation and assembly module for autotransporter export, outer membrane subunit

canonical amino acids at the reassigned codon.[6,21,22] We and others have previously utilized the polyspecificity of the IodoY aaRS synthetase,[23,24] but its ability to charge its cognate tRNA with other nsAAs has not been systematically evaluated. Using the nsAA incorporation kit, we rapidly assessed IodoY OTS polyspecificity (Figure 4c) against a panel of nsAAs that included other halotyrosine derivatives (Figure 2). This system incorporates 3-bromotyrosine, and 3-chlorotyrosine, as efficiently and accurately as it does 3-iodotyrosine. It also incorporates 3-nitrotyrosine, apparently more efficiently and specifically than the halotyrosines. In fact, readthrough of TAG as 3-nitrotyrosine by the IodoY OTS is even more efficient than it was for the NitroY OTS that we tested (Figure 4a). The IodoY OTS may have a very low level of activity for 4-cyanophenylalanine. It appears to have higher fidelity for this nsAA than the CNF aaRS that we tested. The IodoY OTS does not incorporate 4-azidophenylalanine or 3-aminotyrosine.

Amberless *E. coli* Evolved for More Rapid Growth. We tested nsAA incorporation in the amberless *E. coli* strain C321.ΔA.exp in which all TAG amber codons have been replaced with TAA stop codons.[10] This amberless *E. coli* host exhibits a reduced growth rate in minimal media, possibly due to other, unplanned mutations it sustained during its construction. To determine if we could evolve mutants of this strain with restored growth rates, we propagated C321.ΔA.exp over 12 growth cycles, alternating between M9 minimal media and LB. Six populations (N1−N6) were evolved without and six populations (P1−P6) were evolved with the IodoY OTS plasmid. We characterized the growth of five end point clones from different populations (N1, N3, N4, P2 and P3). All of these clones grew much more rapidly than C321.ΔA.exp upon being transferred to M9 media from LB (Figure 5a). There was also less pronounced improvement for strains containing the IodoY OTS plasmid in LB.

We sequenced the genomes of these same five evolved strains to ascertain the mutations that were responsible for their improved growth dynamics (Table 2). Strikingly, every isolate had a mutation affecting the *folA* gene, which encodes dihydrofolate reductase. The five *folA* mutations included two in the promoter region and one stop codon past the conserved part of the protein sequence. Mutations in promoters are rare when there is selection for loss of gene function, so we predict that these mutations lead to an increase in metabolic flux through this enzyme. The two sequenced isolates that evolved with the IodoY OTS also had mutations in *pcnB*, which encodes polyA polymerase I. Mutations in PcnB have previously been shown to reduce the copy number of plasmids with a P15A replication origin,[25] like the OTS plasmid we used. We did not observe any mutations in the sequences of the aaRS or tRNA on the OTS plasmid.

These C321.ΔA.exp variants evolved under conditions in which there was no selection to maintain nsAA incorporation. Given the apparent changes in metabolism and plasmid copy number in the evolved strains, we wondered whether they would exhibit compromised OTS function. We assessed nsAA incorporation in these five strains and an additional isolate (P1) using our kit. We found no change in IodoY OTS efficiency or fidelity in any of the strains evolved with the plasmid present (Figure 5b). By surveying three transformants of the IodoY OTS plasmid into of each of the strains evolved without this plasmid present, we were also able to recover clones with OTS activity similar to that of the ancestral C321.ΔA.exp strain in each case (Figure 5c). The number of apparently defective transformants of each evolved clone is typical of what we saw in constructing other strains with OTS plasmids. In those cases we verified the sequences of the aaRS and tRNA on the OTS plasmid before testing a strain. The current results demonstrate how the nsAA measurement kit can also be useful for identifying transformants with intact OTS function. In conclusion, the growth rate improvements in the evolved variants of amberless *E. coli* do not seem to compromise their nsAA incorporation performance.

Future Improvements to the Kit. Despite the utility of the nsAA measurement kit in its current form, we encountered two aspects of its design that could be improved in future versions. One shortcoming is that mRFP1 signal is low and lags far behind GFP signal. This low signal limits the kit's usefulness for time-resolved studies of OTS performance (*e.g.*, during different growth phases). It occurs despite mRFP1 being translated before sfGFP in the fusion protein. The fact that RFP signal continues to increase for >7 h after cell growth has ceased (Figure 3) indicates that the lag is most likely due to slow maturation of mRFP1 in the context of the fusion protein, even though this mRFP1 variant was selected for rapid monomeric folding.[26] While the mRFP1 signal is not ideal, as long as there is no effect of having nsAA *versus* tyrosine in the linker on RFP (or GFP) maturation time, the relative fluorescence measurements used by the kit will not be affected by this flaw.

After we constructed the kit plasmids, it was reported that the mRFP1 sequence that we used contains a fairly strong internal ribosome binding site (iRBS).[27] In our system, this additional translational start site is expected to create unintended polypeptide products that begin with an N-terminally truncated RFP and then translate normally through the full linker and GFP reading frame. The RBS Calculator (v2.0)[28] predicts that the relative rates of translation from the normal mRFP1 RBS and from the iRBS are 620.33 au and 228.82 au, respectively. Any truncated polypeptides created by translation initiation at the iRBS still monitor readthrough of

DOI: 10.1021/acssynbio.6b00192
ACS Synth. Biol. 2017, 6, 45−54

the test codon, even though they will not have RFP fluorescence. Additionally, we do not expect the relative amount of translation from the normal RBS and the iRBS to vary between the two kit plasmids or between ± nsAA conditions. Therefore, it is unlikely that this iRBS affects the relative measurements made using our kit. But, removing this iRBS by altering mRFP1 codon usage in future versions of the kit plasmids could eliminate this unnecessary complication.

CONCLUSIONS

We have demonstrated that the nsAA measurement kit can be used in a variety of scenarios to evaluate the performance of expanded genetic code systems. Availability of this kit should improve the ability of many researchers to utilize this remarkable technology, including in educational environments with limited access to mass spectrometry. Even for laboratories that do have these resources, we have shown that the kit is a rapid and inexpensive alternative for experiments in which many measurements need to be made: when optimizing the nsAA concentration to use in culture media, when characterizing OTS polyspecificity across many different nsAAs, and when evaluating OTS function in evolved strains containing mutations that improve growth, for example. The kit could be used to evaluate many other variables that affect OTS function in future studies. The effects of varying aaRS and tRNA expression levels, either by using different promoters or plasmid origins, could be examined. Substituting other linkers between the fluorescent proteins in the kit plasmids could be used to test how the efficiency and fidelity of nsAA incorporation depends on the sequence context surrounding the amber codon or to evaluate OTSs that reassign codons other than the amber codon to nonstandard amino acids.

METHODS

Media and Chemicals. Cells were cultured in LB (10 g/L tryptone, 5 g/L yeast extract, 10 g/L NaCl) or in M9 minimal medium supplemented with 1 mg/mL glucose, 1 μg/mL biotin, and 2 μg/mL thiamine (M9GBT). Gentamicin (20 μg/mL), kanamycin (50 μg/mL), zeocin (10 μg/mL) and IPTG (100 μM) were added as appropriate. Amino acids were purchased from Sigma-Aldrich (St. Louis, MO), except *o*-nitrobenzyl-L-tyrosine (Santa Cruz Biotechnology, Dallas, TX), 4-azido-L-phenylalanine (Bachem, Bubendorf, Switzerland), 5-hydroxy-L-tryptophan (Acros Organics, Geel, Belgium), and 4-azido-L-phenylalanine (Chem-Impex, Wood Dale, IL). Stock solutions of L-tyrosine, 3-iodo-L-tyrosine, 4-azido-L-phenylalanine, 3-amino-L-tyrosine, 3-nitro-L-tyrosine, 5-hydroxy-L-tryptophan, and 4-cyano-L-phenylalanine were prepared at 10 mM in dH_2O. For *o*-nitrobenzyl-L-tyrosine a 50 mM stock was prepared in 50% DMSO with the addition of NaOH until the nsAA dissolved. 4-Azido-L-phenylalanine was dissolved at 10 mM in 10% DMSO. L-Tyrosine, 3-iodo-L-tyrosine, and 3-nitro-L-tyrosine were heated to 70 °C to dissolve. All amino acid stocks were sterilized using 0.22 μm filters.

Kit Plasmid Construction. The pRYG (control) and pRXG (assay) plasmids were created from pQE-80L-Kan (Qiagen, Hilden, Germany). This vector contains a pBR322 (ColE1) origin of replication, a kanamycin resistance cassette, the *lacI*^{q} repressor gene, a T5 promoter regulated by *lacO* sites upstream of the cloning site for an open reading frame, and a C-terminal His_6 tag. We began construction with pQE-80L-Kan-sfGFP, a derivative with superfolder GFP[29] cloned into pQE-80L-Kan. The coding sequence for mRFP1[26] was amplified from the E1010 BioBrick plasmid with Phusion polymerase and digested with DpnI. The PCR primers used at this step appended the linker sequence[30] containing the TAC or TAG test codon and introduced DNA sequence overlaps for Gibson assembly[31] into pQE-80L-Kan-sfGFP. Assembly reactions were transformed into TOP10 *E. coli* (Invitrogen), and the kit plasmids were Sanger sequenced for verification. All enzymes for cloning were purchased from New England Biolabs (Ipswich, MA).

OTS Plasmids. Each OTS system was constructed by using Gibson assembly to clone the respective aaRS mutant (Table 1) into plasmid pRF0G, a derivative of pRF0S in which spectinomycin resistance was replaced with gentamicin resistance. The pRF0S plasmid has been described previously.[23] Briefly, it is organized as follows. Each pRF0G plasmid includes a p15A origin of replication, and the respective OTS aaRS is expressed from a copy of the native *E. coli* TyrRS promoter. The aaRS is followed by a colinear downstream copy of the nap3 tRNA[32] expressed from the *lpp* promoter, and both transcripts are terminated by an *rrnB* terminator. In place of nap3, the 5HTP OTS plasmid contains the 40A variant of the AS3.4 tRNA.[12]

Incorporation Assays. Each OTS plasmid was transformed separately into *E. coli* strain C321.ΔA.exp (AddGene: #49018)[10] cells already containing either pRYG or pRXG that were made electrocompetent by 10% glycerol washes. The corresponding nonstandard amino acid was added at 250 μM in the SOC media used during recovery, in the LB agar used for plating to pick transformants, and in all subsequent liquid cultures of the strain before testing. We Sanger sequenced the aaRS and tRNA genes in these clones to verify that no mutations had occurred in the OTS cassette prior to testing them using the nsAA incorporation measurement kit.

For kit assays, strains were revived from −80 °C glycerol stocks in 10 mL LB in 50 mL Erlenmeyer flasks with kanamycin, zeocin, gentamicin, and the relevant amino acid. These cultures were incubated at 37 °C with orbital shaking over a 1-in. diameter at 225 rpm for 24 h. Then, 10 μL of each revived culture were transferred into 10 mL of fresh media and again incubated for 24 h. From these preconditioned cultures, a diluted culture was prepared by concentrating cells in 500 μL of culture by centrifugation at 4 °C, decanting the supernatant, and then adding 10 mL of fresh media with antibiotics IPTG and ± nsAA. This procedure creates an overall 1:20 dilution in fresh media. Cultures lacking nsAA were supplemented with an equivalent amount of sterile dH_2O water to achieve a consistent LB concentration. Sample blanks ± nsAA were prepared in an identical way, but omitting cells.

Fluorescence and OD readings were made in using an Infinite M200 PRO microplate reader (Tecan, Zürich, Switzerland). For each experiment, a Costar #3631 black clear-bottom 96-well plate was filled with 200 μL aliquots of each sample and blank to be tested. The assay was run for 14 h in the microplate reader while it was incubated continuously at 37 °C and shaken 15 s before and after readings. OD, RFP, and GFP measurements were taken every 12 min. OD was measured at 600 nm (OD600). The RFP excitation wavelength was set at 550 nm with an emission wavelength at 675 nm, and GFP excitation was set at 480 nm with emission at 525 nm.

Calculation of RRE and MMF Values. Data analysis and visualization were performed using the R Statistical Programming Language. Scripts and raw data used in this study are

DOI: 10.1021/acssynbio.6b00192
ACS Synth. Biol. 2017, 6, 45−54

freely available online (http://github.com/barricklab/nsAA-kit). For data at each collected time point, the analysis pipeline: (1) subtracts ± nsAA media blank values, as appropriate, from the signal in every well, (2) normalizes RFP and GFP fluorescent signals to the OD600 in each well, and then (3) calculates RRE and MMF values using the equations in Figure 1. The steps in this series of calculations are illustrated for several OTSs in Figure 3.

For condensing this information into a single estimate of RRE and MMF during log phase (as shown in Figure 4), each replicate set of measurements consisting of four wells (pRYG ± nsAA and pRXG ± nsAA) was analyzed to find the time window when the average OD600 across these four wells was within the mid log range from 0.3 to 0.4. The RRE and MMF values determined for each of these sets of four wells at each time point were then averaged over this time window to create summary scores for that replicate.

For the tests of different OTSs, we compared three technical replicates, all derived from the same preconditioned culture, of each of six different transformants of the pRF0G aaRS-tRNA plasmids into strains containing pRYX and pRYG (9 sets of measurements, consisting of 36 total wells, plus 6 additional blank wells). In some cases, outlier replicates that had erratic or lower performance were removed. Because variation between technical replicates was so great that it masked any variation between the biological replicates, we pooled all RRE and MMF values and treated them as technical replicates to estimate 95% confidence intervals. The test of 4-azido-L-phenylalanine concentration used five technical replicates of each of the seven concentrations tested, with blanks at each concentration of nsAA. The polyspecificity test of the IodoY OTS used three replicates of each of the eight nsAA treatments.

Protein Purification and Mass Spectrometry. Strains were revived and preconditioned as described for incorporation assays. Then, 2.5 mL of overnight preconditioned culture was inoculated into 50 mL fresh LB with IPTG in each of two 250 mL Erlenmeyer flasks. Cells were harvested from these cultures after growth to stationary phase (~24 h) by concentrating the entire cultures by centrifugation at 4 °C, decanting the media, and flash freezing the resulting cell pellets using liquid nitrogen for storage at −80 °C. All growth steps included 250 μM nsAA.

Pellets were thawed on ice and resuspended in lysis buffer (50 mM NaH_2PO_4, 300 mM NaCl, 10 mM imidazole, pH 8.0) with 1 mg/mL lysozyme, 1× HALT Protease Inhibitor Cocktail without EDTA (ThermoFisher) and 1250 U of benzonase nuclease (Sigma-Aldrich). Samples were incubated at 37 °C for 30 min and then clarified by centrifugation at 12 000 RCF for 20 min. Clarified lysates were then transferred to plastic gravity chromatography columns, combined with Ni-NTA agarose (Qiagen) and allowed to bind 1 h at room temperature on a rotating platform. Protein-bound resin was sandwiched between two fritted discs in the chromatography column, the remaining unbound protein fraction was allowed to drain, and the resin washed once with 5 column volumes (CV) of wash buffer #1 (50 mM NaH_2PO_4, 300 mM NaCl, 10 mM imidazole, pH 8.0), twice with 20 CV of wash buffer #2 (50 mM NaH_2PO_4, 500 mM NaCl, 10 mM imidazole, pH 8.0), and eluted in 250 μL fractions with elution buffer (50 mM NaH_2PO_4, 500 mM NaCl, 250 mM imidazole, pH 8.0). Fractions with highest concentration of protein (measured by GFP fluorescence) were combined, and lysate, unbound protein, wash, and elution fractions were analyzed by SDS-PAGE electrophoresis to determine purity. Purified proteins were exchanged into 0.1% formic acid by three rounds of centrifugal ultrafiltration and resuspension into 500 uL 0.1% formic acid using Amicon Ultra-4 filters with a MWCO of 10 kDa (Millipore, Billerica, MA). Intact protein masses were determined by LC ESI-MS using an Orbitrap Elite (Thermo-Fisher) connected to a Dionex 3000 nanospray UPLC at the University of Texas at Austin Proteomics Core Facility.

Amberless *E. coli* Evolution Experiment. Twelve populations of *E. coli* C321.ΔA.exp—six carrying pRF0G encoding the IodoY OTS (designated P1−P6) and six with no plasmid (designated N1−N6)—were initiated from single colonies. Each population was propagated through 12 cycles of 1:1000 dilution and regrowth to saturation in 10 mL of media in 50 mL Erlenmeyer flasks. Growth cycles alternated between LB for 24 h and M9GBT for 48 h. Zeocin was added to all cultures. Gentamicin and 100 μM 3-iodo-L-tyrosine were added to populations with the IodoY OTS. At the end of the experiment, each population was diluted and plated on LB agar with appropriate supplements to pick one clonal isolate for further study.

We sequenced the genomes of five evolved clones from different populations (N1, N3, N4, P2, P3) and the unevolved N and P clones. Genomic DNA was purified from overnight cultures of each strain using the PureLink Genomic DNA Mini Kit (Invitrogen, Carlsbad, CA) and processed with the KAPA LTP Library Preparation Kit for Illumina platforms (Kapa Biosystems, Wilmington, MA). The resulting libraries were sequenced on an Illumina HiSeq 2500 at the University of Texas at Austin Genome Sequencing and Analysis Facility to generate paired-end 125-base reads. We predicted the mutations present in each clone by comparing these reads to the C321.ΔA genome (GenBank:CP006698.1)[10] using *breseq* (version 0.26.1).[33] FASTQ read files have been deposited in the NCBI Sequence Read Archive (accession SRP065568).

We monitored growth of evolved strains by reviving *E. coli* K-12 MG1655, C321.ΔA.exp, N1, N3, N4, P2, and P3 in 10 mL of LB in 50 mL flasks overnight at 37 °C with shaking at 225 rpm. All cultures were supplemented with zeocin except for MG1655. P1, P2, and P3 were additionally supplemented with gentamicin and 100 μM 3-iodo-L-tyrosine. Each culture was preconditioned by making a 1:100 dilution of the revived culture into 10 mL fresh LB containing the same supplements for each strain. After growth for 24 h under the same conditions, another 1:100 dilution was made into LB or M9GBT medium with the same supplements. OD600 was monitored by removing samples of each culture over 24 or 48 h.

■ ASSOCIATED CONTENT

Supporting Information

The Supporting Information is available free of charge on the ACS Publications website at DOI: 10.1021/acssynbio.6b00192.

Protein mass spectrometry results for the mRFP1-sfGFP fusion protein expressed from the nsAA kit assay plasmid using the Tyr, IodoY, NitroY, AminoY, and CNF OTSs. (PDF)

■ AUTHOR INFORMATION

Corresponding Authors

*E-mail: dennis.mishler@gmail.com.
*E-mail: jbarrick@cm.utexas.edu.

DOI: 10.1021/acssynbio.6b00192
ACS Synth. Biol. 2017, 6, 45−54

Author Contributions

J.W.M., M.J.H., C.M., A.E.G., N.Y.S., E.W., and D.M.M. designed, constructed, and tested kit plasmids. M.J.H. and S.P.L. created aaRS-tRNA plasmids. C.W.B. purified proteins and analyzed mass spectrometry results. S.P.L. performed the C321.ΔA.exp evolution experiment. C.W.B. and S.P.L. measured growth curves of evolved strains. S.P.L. and J.E.B. analyzed genome resequencing data. All authors wrote and edited the manuscript.

Notes

The authors declare no competing financial interest.

■ ACKNOWLEDGMENTS

We thank Michelle Byrom and Jimmy Gollihar for technical assistance; and Marc Lajoie and George Church for providing strain C321.ΔA.exp. We acknowledge the Texas Advanced Computing Center (TACC) at the University of Texas at Austin for providing high-performance computing resources. We thank the UT Austin Center for Systems and Synthetic Biology, Institute for Cellular and Molecular Biology, and Department of Molecular Biosciences for their support of the 2014 UT Austin iGEM team. This research was supported the Welch Foundation (F-1780) and the NSF BEACON Center for the Study of Evolution (DBI-0939454).

■ ABBREVIATIONS

aaRS, aminoacyl-tRNA synthetase; MMF, maximum misincorporation frequency; nsAA, nonstandard amino acid; OTS, orthogonal translation system; RRE, relative readthrough efficiency

■ REFERENCES

(1) Benner, S. A., and Sismour, A. M. (2005) Synthetic biology. *Nat. Rev. Genet. 6*, 533−43.
(2) O'Donoghue, P., Ling, J., Wang, Y.-S., and Söll, D. (2013) Upgrading protein synthesis for synthetic biology. *Nat. Chem. Biol. 9*, 594−598.
(3) Liu, C. C., and Schultz, P. G. (2010) Adding new chemistries to the genetic code. *Annu. Rev. Biochem. 79*, 413−444.
(4) Sakamoto, K., Murayama, K., Oki, K., Iraha, F., Kato-Murayama, M., Takahashi, M., Ohtake, K., Kobayashi, T., Kuramitsu, S., Shirouzu, M., and Yokoyama, S. (2009) Genetic encoding of 3-iodo-L-tyrosine in *Escherichia coli* for single-wavelength anomalous dispersion phasing in protein crystallography. *Structure 17*, 335−244.
(5) Voth, A. R., Khuu, P., Oishi, K., and Ho, P. S. (2009) Halogen bonds as orthogonal molecular interactions to hydrogen bonds. *Nat. Chem. 1*, 74−79.
(6) Liu, T., Wang, Y., Luo, X., Li, J., Reed, S. A., Xiao, H., Young, T. S., and Schultz, P. G. (2016) Enhancing protein stability with extended disulfide bonds. *Proc. Natl. Acad. Sci. U. S. A. 113*, 5910−5915.
(7) Nikić, I., Kang, J. H., Girona, G. E., Aramburu, I. V., and Lemke, E. A. (2015) Labeling proteins on live mammalian cells using click chemistry. *Nat. Protoc. 10*, 780−791.
(8) Chin, J. W., Martin, A. B., King, D. S., Wang, L., and Schultz, P. G. (2002) Addition of a photocrosslinking amino acid to the genetic code of *Escherichia coli*. *Proc. Natl. Acad. Sci. U. S. A. 99*, 11020−11024.
(9) Deiters, A., Groff, D., Ryu, Y., Xie, J., and Schultz, P. G. (2006) A genetically encoded photocaged tyrosine. *Angew. Chem., Int. Ed. 45*, 2728−2731.
(10) Lajoie, M. J., Rovner, A. J., Goodman, D. B., Aerni, H.-R., Haimovich, A. D., Kuznetsov, G., Mercer, J. A., Wang, H. H., Carr, P. A., Mosberg, J. A., Rohland, N., Schultz, P. G., Jacobson, J. M., Rinehart, J., Church, G. M., and Isaacs, F. J. (2013) Genomically recoded organisms expand biological functions. *Science 342*, 357−360.
(11) Haruna, K., Alkazemi, M. H., Liu, Y., Söll, D., and Englert, M. (2014) Engineering the elongation factor Tu for efficient selenoprotein synthesis. *Nucleic Acids Res. 42*, 9976−9983.
(12) Ellefson, J. W., Meyer, A. J., Hughes, R. A., Cannon, J. R., Brodbelt, J. S., and Ellington, A. D. (2014) Directed evolution of genetic parts and circuits by compartmentalized partnered replication. *Nat. Biotechnol. 32*, 97−101.
(13) Amiram, M., Haimovich, A. D., Fan, C., Wang, Y.-S., Ntai, I., Moonan, D. W., Ma, N. J., Rovner, A. J., Hoon, S., Kelleher, N. L., Goodman, A. L., Jewett, M. C., Söll, D., Rinehart, J., and Isaacs, F. J. (2015) Evolution of translation components in recoded organisms enables multi-site nonstandard amino acid incorporation in proteins at high yield and purity. *Nat. Biotechnol. 33*, 1272−1278.
(14) Antonczak, A. K., Morris, J., and Tippmann, E. M. (2011) Advances in the mechanism and understanding of site-selective noncanonical amino acid incorporation. *Curr. Opin. Struct. Biol. 21*, 481−487.
(15) Antonczak, A. K., Simova, Z., Yonemoto, I. T., Bochtler, M., Piasecka, A., Czapinska, H., Brancale, A., and Tippmann, E. M. (2011) Importance of single molecular determinants in the fidelity of expanded genetic codes. *Proc. Natl. Acad. Sci. U. S. A. 108*, 1320−1325.
(16) Wang, L., Brock, A., Herberich, B., and Schultz, P. G. (2001) Expanding the genetic code of *Escherichia coli*. *Science 292*, 498−500.
(17) Mukai, T., Hayashi, A., Iraha, F., Sato, A., Ohtake, K., Yokoyama, S., and Sakamoto, K. (2010) Codon reassignment in the *Escherichia coli* genetic code. *Nucleic Acids Res. 38*, 8188−8195.
(18) Hammerling, M. J., Ellefson, J. W., Boutz, D. R., Marcotte, E. M., Ellington, A. D., and Barrick, J. E. (2014) Bacteriophages use an expanded genetic code on evolutionary paths to higher fitness. *Nat. Chem. Biol. 10*, 178−180.
(19) Chin, J. W., Santoro, S. W., Martin, A. B., King, D. S., Wang, L., and Schultz, P. G. (2002) Addition of *p*-azido-L-phenylalanine to the genetic code of *Escherichia coli*. *J. Am. Chem. Soc. 124*, 9026−9027.
(20) Rovner, A. J., Haimovich, A. D., Katz, S. R., Li, Z., Grome, M. W., Gassaway, B. M., Amiram, M., Patel, J. R., Gallagher, R. R., Rinehart, J., and Isaacs, F. J. (2015) Recoded organisms engineered to depend on synthetic amino acids. *Nature 518*, 89−93.
(21) Young, D. D., Young, T. S., Jahnz, M., Ahmad, I., Spraggon, G., and Schultz, P. G. (2011) An evolved aminoacyl-tRNA synthetase with atypical polysubstrate specificity. *Biochemistry 50*, 1894−1900.
(22) Guo, L., Wang, Y., Nakamura, A., Eiler, D., Kavran, J. M., Wong, M., Kiessling, L. L., Steitz, T. A., O'Donoghue, P., and Söll, D. (2014) Polyspecific pyrrolysyl-tRNA synthetases from directed evolution. *Proc. Natl. Acad. Sci. U. S. A. 111*, 16724−16729.
(23) Hammerling, M. J., Gollihar, J., Mortensen, C., Alnahhas, R. N., Ellington, A. D., and Barrick, J. E. (2016) Expanded genetic codes create new mutational routes to rifampicin resistance in *Escherichia coli*. *Mol. Biol. Evol. 9*, 2054.
(24) Tack, D. S., Ellefson, J. W., Thyer, R., Wang, B., Gollihar, J., Forster, M. T., and Ellington, A. D. (2016) Addicting diverse bacteria to a noncanonical amino acid. *Nat. Chem. Biol. 12*, 138−140.
(25) Liu, J. D., and Parkinson, J. S. (1989) Genetics and sequence analysis of the *pcnB* locus, an *Escherichia coli* gene involved in plasmid copy number control. *J. Bacteriol. 171*, 1254−1261.
(26) Campbell, R. E., Tour, O., Palmer, A. E., Steinbach, P. A., Baird, G. S., Zacharias, D. A., and Tsien, R. Y. (2002) A monomeric red fluorescent protein. *Proc. Natl. Acad. Sci. U. S. A. 99*, 7877−7882.
(27) Whitaker, W. R., Lee, H., Arkin, A. P., and Dueber, J. E. (2015) Avoidance of truncated proteins from unintended ribosome binding sites within heterologous protein coding sequences. *ACS Synth. Biol. 4*, 249−257.
(28) Espah Borujeni, A., Channarasappa, A. S., and Salis, H. M. (2014) Translation rate is controlled by coupled trade-offs between site accessibility, selective RNA unfolding and sliding at upstream standby sites. *Nucleic Acids Res. 42*, 2646−2659.
(29) Pédelacq, J.-D., Cabantous, S., Tran, T., Terwilliger, T. C., and Waldo, G. S. (2006) Engineering and characterization of a superfolder green fluorescent protein. *Nat. Biotechnol. 24*, 79−88.

DOI: 10.1021/acssynbio.6b00192
ACS Synth. Biol. 2017, 6, 45−54

(30) Waldo, G. S., Standish, B. M., Berendzen, J., and Terwilliger, T. C. (1999) Rapid protein-folding assay using green fluorescent protein. *Nat. Biotechnol. 17*, 691−695.
(31) Gibson, D. G., Young, L., Chuang, R.-Y., Venter, J. C., Hutchison, C. A., and Smith, H. O. (2009) Enzymatic assembly of DNA molecules up to several hundred kilobases. *Nat. Methods 6*, 343−345.
(32) Guo, J., Melançon, C. E., Lee, H. S., Groff, D., and Schultz, P. G. (2009) Evolution of amber suppressor tRNAs for efficient bacterial production of proteins containing nonnatural amino acids. *Angew. Chem., Int. Ed. 48*, 9148−9151.
(33) Deatherage, D. E., and Barrick, J. E. (2014) Identification of mutations in laboratory-evolved microbes from next-generation sequencing data using *breseq*. *Methods Mol. Biol. 1151*, 165−188.
(34) Zwietering, M., Jongenburger, I., Rombouts, F., and van't Riet, K. (1990) Modeling of the bacterial growth curve. *Appl. Environ. Microbiol. 56*, 1875−1881.
(35) Seyedsayamdost, M. R., Xie, J., Chan, C. T. Y., Schultz, P. G., and Stubbe, J. (2007) Site-specific insertion of 3-aminotyrosine into subunit α2 of *E. coli* ribonucleotide reductase: direct evidence for involvement of Y730 and Y731 in radical propagation. *J. Am. Chem. Soc. 129*, 15060−15071.
(36) Neumann, H., Hazen, J. L., Weinstein, J., Mehl, R. A., and Chin, J. W. (2008) Genetically encoding protein oxidative damage. *J. Am. Chem. Soc. 130*, 4028−2033.
(37) Schultz, K. C., Supekova, L., Ryu, Y., Xie, J., Perera, R., and Schultz, P. G. (2006) A genetically encoded infrared probe. *J. Am. Chem. Soc. 128*, 13984−13985.

DOI: 10.1021/acssynbio.6b00192
ACS Synth. Biol. 2017, 6, 45−54